

Broadband-matching of Coupled Inductive Loops Used for Vehicle Communications

KARL HEINZ KRAFT

Faculty of Electrical Engineering,
Ostfalia University of Applied Sciences,
Salzdahlumer Str. 46-48, D-38302 Wolfenbüttel,
GERMANY

Abstract: - Safe and effective data communications systems are important components for modern traffic management. The transmission of information between vehicles and wayside equipment is required for railway systems, for management of road traffic and for control of transportation within factories. The application of inductive loops is well-known for all the named cases using different dimensions, frequencies and data transmission rates. A general approach seems to be useful in order to develop a design strategy taking into account the magnetic field, the geometric properties, the required transmission rate and therefore the bandwidth and structure of the filters to be used. The developed procedure delivers an optimized filter design based on the frequency-depending power transfer.

Key-Words: - Traffic management, data transmission, inductive loops, magnetic field strength, filter design, band-pass filters, broadband-matching, transmitted power, SPICE.

Received: May 22, 2024. Revised: November 13, 2024. Accepted: March 6, 2025. Published: June 6, 2025.

1 Introduction

The design of data transmission devices based on coupled inductive loops used for vehicle control in transportation systems is a rather complicated task because several parameters and their dependencies must be taken into account. A suitable solution has to be matched to the properties of the specific traffic conditions, e.g. with a view on high-speed railways, urban traffic or internal transportation systems within factory plants. A symbolic simplified representation of the system is depicted in Figure 1. Several tasks can be named: determination of the generated magnetic field strength as a function of the position above the loop, calculation and measurement of self and mutual inductance, design of band-pass filters with regard to bandwidth, centre-frequency and impedance transformation. The coupling of the loops is another problem, not only because of the power transfer and the required output voltage of the transmitter but also because of the resulting filter characteristic.

2 Problem Formulation

The frequency-depending behaviour of the transmission system can be described by an equivalent circuit consisting of all relevant

elements. An ac-analysis is possible as well as the simulation of the transient behaviour, preferably with a software tool, e.g. SPICE.

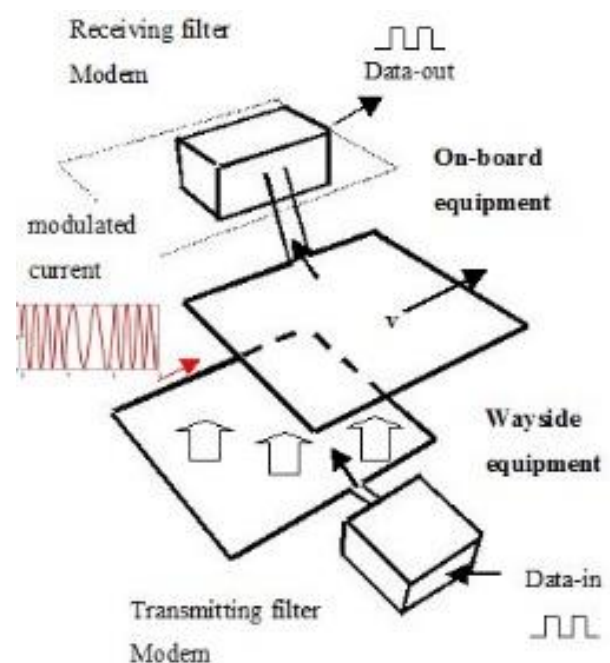


Fig. 1: Architecture of the system

Several papers may be mentioned in the field of data communications, for instance [1], [2], [3], [4], [5] with traffic control applications, and

furthermore [6], [7], [8] concerning NFC and wireless power transfer. [1] gives an overview on the European train control system, [2] explains the EURO-Balise. The focus here lies on the ac-behaviour which alone is rather complicated, although transient responses would be interesting as well. Loop occupation times are calculated for example in [4].

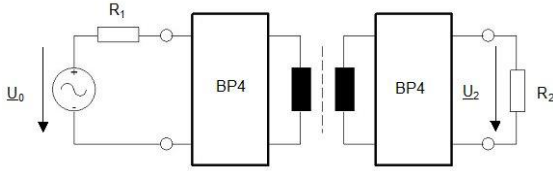


Fig. 2: Equivalent circuit of the investigated configuration

Figure 2 shows the mentioned equivalent circuit. To reduce the number of parameters, two equal quadratic loops, each with one winding, are considered. They are connected with identical band-pass filters (input and output exchanged).

3 Inductances

In order to find plausible parameters concerning the magnetic field, the loop inductance and the mutual inductance of two coupled loops, it is sufficient to use some approximations, because the main objective is the filter design procedure. Other aspects such as different loop geometries, the influence of the neighbourhood and edge effects would be interesting, of course, but are not investigated here.

The generated magnetic field strength of a rectangular inductive loop (length l , in relation to the direction x of a moving vehicle, width a , diameter D of the wire, $d \ll a, l$) can be calculated via the law of Biot-Savart. The extensive final result $H_z(x)$ in (5) has been divided into four supporting equations (1-4). The position $x=0, y=0, z=0$ marks the exact centre of the loop, the height $z=h$ gives the distance above (or below) the loop, and the loop current may be I_0 . For a square-shaped loop, we set $l=a$.

The distance h is important with a view on the mutual inductance $M=L_{12}$ in combination with a second loop. An example $H_z(x, h)$ is shown in Figure 3 for the case $a=l=40$ cm, $I_0=1$ A. The choice of the length a is essential concerning the self-inductance L_a and the mutual inductance M .

$$A_{z1}(x) = \frac{1}{\left(\frac{a}{2}\right)^2 + h^2} + \frac{1}{\left(\frac{l}{2} - x\right)^2 + h^2}, \quad (1)$$

$$A_{z2}(x) = \frac{\frac{l}{2} - x}{\sqrt{\left(\frac{l}{2} - x\right)^2 + \left(\frac{a}{2}\right)^2 + h^2}} \quad (2)$$

$$A_{z3}(x) = \frac{1}{\left(\frac{a}{2}\right)^2 + h^2} + \frac{1}{\left(\frac{l}{2} + x\right)^2 + h^2}, \quad (3)$$

$$A_{z4}(x) = \frac{\frac{l}{2} + x}{\sqrt{\left(\frac{l}{2} + x\right)^2 + \left(\frac{a}{2}\right)^2 + h^2}} \quad (4)$$

$$H_z(x) = \frac{I_0 \cdot a}{4 \cdot \pi} \cdot [A_{z1}(x) \cdot A_{z2}(x) + A_{z3}(x) \cdot A_{z4}(x)]. \quad (5)$$

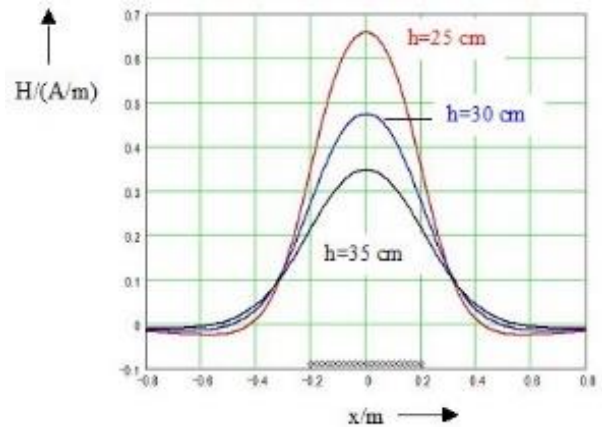


Fig. 3: Magnetic field-strength $H_z(x)$ above the inductive loop

Several formulae may be used to estimate the inductance L_a of a rectangular inductive loop, e.g. (6) according to [9]:

$$L_a \approx \frac{2 \cdot \mu_0 \cdot a}{\pi} \cdot \left[\operatorname{arsinh} \frac{2 \cdot a}{d} - 1 \right]. \quad (6)$$

A special value is given by $L_a \approx 1.75 \mu\text{H}$ with $a=40$ cm and $d=2.5$ mm. The evaluation of (6) shows the result $L_a \sim a$ using plausible parameters with a view on the tasks at hand. Furthermore, the mutual inductance of two identical loops with distance h can be calculated via the magnetic flux: $\Phi = \int \mu_0 \cdot H \cdot dA = M \cdot I_0$. The calculated result (7) here:

$$M(a, h) \approx \frac{\mu_0 \cdot a}{2 \cdot \pi} \cdot \frac{\left(\frac{a}{h}\right)^3}{\left(1 + \frac{1}{4} \cdot \left(\frac{a}{h}\right)^2\right) \cdot \sqrt{1 + \frac{1}{2} \cdot \left(\frac{a}{h}\right)^2}}. \quad (7)$$

For the following discussion, the value $M \approx 0.1 \mu\text{H}$ will be used ($a=40 \text{ cm}$, $h=0.27 \text{ cm}$, $L=1.8 \mu\text{H}$). The coupling factor is given by $k=M/L=0.055$. From (7) can be concluded that a relatively high ratio of a/h seems to be advantageous, on the other hand, there are disadvantages with respect to bandwidth and impedance matching if higher values of L_a are used. The choice of suitable dimensions (a , h) for a specific application must take into account the proposed frequency range. An equivalent circuit with a coupling of two loops is shown in Figure 4, the calculated voltage transfer function is given by (8)

$$F_c(p) = \frac{U_2(p)}{U_0(p)} = \frac{p \cdot \frac{M}{R_1}}{p^2 \cdot \frac{L_1 \cdot L_2 - M^2}{R_1 \cdot R_2} + p \cdot \left(\frac{L_1}{R_1} + \frac{L_2}{R_2}\right) + 1} \quad (8)$$

with the complex frequency $p = \sigma + j \cdot \omega$.

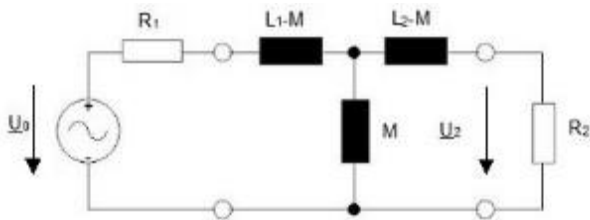


Fig. 4: Equivalent circuit for the coupling of two inductive loops

This band-pass function of 2nd order possesses the maximum value (magnitude) $F_{cm} = M / (2 \cdot L)$ under the conditions $R = R_1 = R_2$, $L = L_1 = L_2$, the corresponding frequency is $f_m = R / (2 \cdot \pi \cdot L)$.

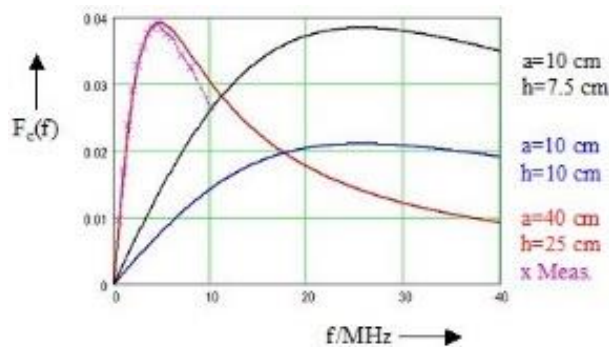


Fig. 5: Magnitude of the voltage transfer function with parameters a and h , and with measured values

In addition, (8) can also be used to determine the mutual inductance M . By variation of a and h and evaluating $|F_c(f)|$, the relations between the relevant parameters become apparent, examples can be seen in Figure 5, including measured values, gained by voltage measurements for comparison,

and with good accordance. The calculated mutual inductance for the case $a=40 \text{ cm}$, $h \approx 25 \text{ cm}$, $L=1.8 \mu\text{H}$ is $M = 2 \cdot L \cdot F_{cm} = 0.14 \mu\text{H}$ with $f_m = 4.4 \text{ MHz}$. This way, the design procedure can be prepared, and the next important step is the filter design.

4 Filter Design

4.1 One Single Band-Pass

The schematics of the band-pass dedicated to the transmitter are shown in Figure 6. The properties of the inductive loop are represented by the elements R_a and L_a , both can be measured and approximately calculated as demonstrated above. It has to be emphasized that one degree of freedom is missing in comparison to the classical filter design because L_a is already fixed by the dimensions of the loop.

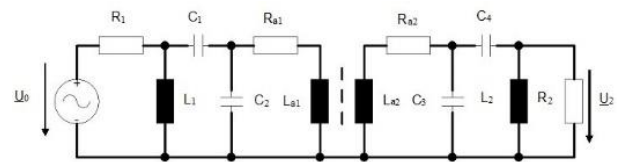


Fig. 6: Schematic of the complete circuit

A fundamental task is the design of a 4th-order band-pass (BP4), ignoring at first the inductive coupling.

The entire circuit can later be investigated. The following steps are necessary for the dimensioning of the BP4-subcircuit: 1) Estimation of the performance by the specification of a suitable filter curve and using the Bode-integral [5], [10]; including the required bandwidth, for instance concerning the Butterworth-characteristic. 2) Development of design equations based on a reference low-pass of 2nd order, application of the frequency- and the Norton-transformation, [5], [11]. The result is the impedance-transforming band-pass shown in Figure 6, without serial and parallel resonant circuits as required. 3) However, the demanded bandwidth will narrowly be missed because of the fixed element L_a , but a correction is possible by decreasing the power transfer ratio $g_0^2 = |S_{21}(f_0)|^2$ at the centre-frequency f_0 or by increasing the input reflection factor $\rho_0 = \sqrt{1 - g_0^2}$. This is possible by the use of the equations listed below and an approximation of the demanded bandwidth. The relevant value of the loop-resistance R_a has to be calculated via an expression with respect to the skin effect using the following parameters: diameter d of a wire with circular profile (e.g. $d=1.8 \text{ mm}$), specific conductance

$\kappa=57 \cdot 10^6 \text{ 1}/(\Omega \cdot \text{m})$, magnetic field constant $\mu_0=4 \cdot \pi \cdot 10^{-7} \text{ V} \cdot \text{s}/(\text{A} \cdot \text{m})$. The depth of penetration is given by $\delta=1/\sqrt{(\pi \cdot \mu_0 \cdot \kappa \cdot f)}$, the resistance per length by $R'=1/(\kappa \cdot A)$, and the profile area by $A=\pi \cdot (d/2)^2$. Summarizing we find the following formula (9) with loop circumference $4 \cdot a$ and with a suitable reference frequency f_{ref} :

$$R_a = \frac{4 \cdot a}{\kappa \cdot \pi \cdot d \cdot \delta} = \frac{4 \cdot a}{d} \cdot \sqrt{\frac{\mu_0 \cdot f_{\text{ref}}}{\pi \cdot \kappa}} \cdot \sqrt{\frac{f}{f_{\text{ref}}}} \quad (9)$$

The Bode-integral is defined by (10), using the bandwidth B , the time constant $\tau_a=L_a/R_a$ and the reflection factor $\underline{S}_{11}(\omega)$:

$$2 \cdot \int_0^{\infty} \ln\left(\frac{1}{|\underline{S}_{11}|}\right) d\omega = \frac{2 \cdot \pi}{\tau_a} \quad (10)$$

The parameter g_0 here with $n=2$ is given by (11)

$$g_0^2 = 1 - \left[1 - \frac{\sin\left(\frac{\pi}{2 \cdot n}\right)}{\pi \cdot \tau_a \cdot B} \right]^{2 \cdot n} \quad (11)$$

the transformation ratio by (12)

$$w = \sqrt{\frac{R_1}{R_a} \cdot \frac{1 - \rho_0}{1 + \rho_0}} \quad (12)$$

The reference values are defined by $R_{\text{ref}}=R_a$, $f_{\text{ref}}=f_0$, $L_{\text{ref}}=R_{\text{ref}}/(2 \cdot \pi \cdot f_{\text{ref}})$, $C_{\text{ref}}=1/(R_{\text{ref}} \cdot 2 \cdot \pi \cdot f_{\text{ref}})$. The values of the circuit elements can be expressed by (13-15):

$$L_1 = \frac{w^2}{w-1} \cdot L_a \quad (13)$$

$$C_2 = \frac{1}{w} \cdot \frac{L_B}{L_a} \cdot C_B \quad (14)$$

$$C_3 = \frac{w-1}{w} \cdot \frac{L_B}{L_a} \cdot C_B \quad (15)$$

The design procedure becomes clear: increasing the value of reflection factor ρ_0 until the desired bandwidth B_0 has been reached for the calculated or simulated filter curve. It must be kept in mind that the accessible data rate depends on the bandwidth of the transmission channel. A complete example with all parameters may support the proposed method. A widely used modulation technique is FSK (Frequency Shift Keying), a data transmission rate of e.g. $r_D=200 \text{ kbit/s}$ requires $B_0 \approx 200 \text{ kHz}$ which can be proved by looking at the generated spectrum. With $f_0=2.3 \text{ MHz}$, $a=40 \text{ cm}$, $L_a=1.8 \text{ } \mu\text{H}$, $R_a=0.27 \text{ } \Omega$, $\rho_0=0.69$, $g_0^2=0.523$ the following result will be found for the BP4: $w=5.819$, $L_1=12.7 \text{ } \mu\text{H}$, $C_2=457 \text{ pF}$, $C_3=2.2 \text{ nF}$, whereby $B=157 \text{ kHz}$ fails the agreement $B \geq B_0$. The

mentioned iteration steps deliver finally $\rho_0=0.76$, $g_0^2=0.422$, $w=5.03$, $L_1=11.3 \text{ } \mu\text{H}$, $C_2=529 \text{ pF}$, $C_3=2.13 \text{ nF}$ and $B=204 \text{ kHz}$.

4.2 Two Coupled Band-Passes

Another correction is necessary if two coupled band-passes will be used for the transmission system. It should be noted that different port resistances have to be used for the BP4 (R_a , R_2) and for the complete circuit (R_1 , R_2). The final result with the coupling factor $k=0.05$ has the following values: $\rho_0=0.8$, $g_0^2=0.496$, $w=4.54$, $L_1=L_6=10.5 \text{ } \mu\text{H}$, $C_2=C_5=586 \text{ pF}$, $C_3=C_4=2.07 \text{ nF}$ and $B=205 \text{ kHz}$. The appertaining filter curve can be seen in Figure 7 using the power transfer function $S_{21}^2(f)=P_2(f)/P_{1\text{max}}$ with the maximum power $P_{1\text{max}}=U_0^2/(4 \cdot R_1)$ and three values of the coupling factor k . Not only the power transfer depends on k , but also the shape of the filter curve. Some measurement values are shown additionally. Of course, there are deviations from the theoretical values because of the rounded elements values. The practical realization requires some fine-tuning.

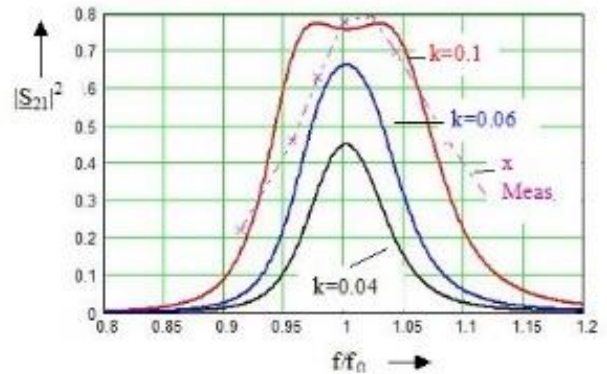


Fig. 7: Frequency-depending power transfer ($f_0=2.3 \text{ MHz}$, $a=40 \text{ cm}$, various distances, resp. coupling factors, measurement values)

The influence of the coupling on the (transmitting) filter becomes apparent if the frequency-depending output impedance has been computed. By looking at the schematics (Figure 6), it is clear that the voltage over C_3 and the current through R_{a1} are relevant. Evaluation of the complex impedance \underline{Z}_{a1} shows that the imaginary part is quasi-linear, while the real part changes substantially within the pass-band of the filter (Figure 8).

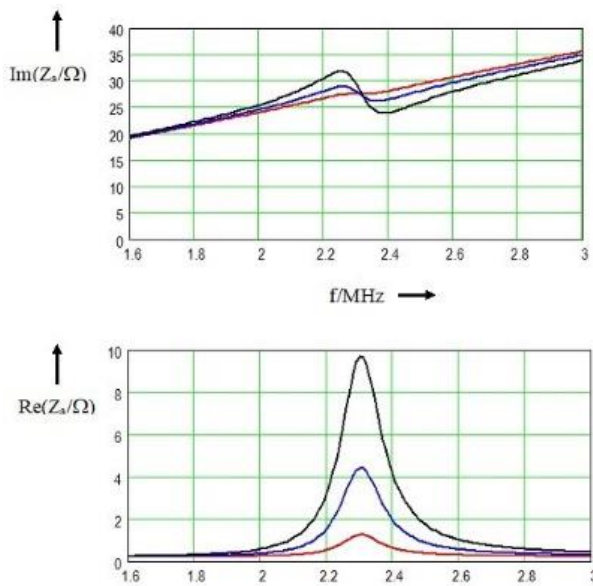


Fig. 8: Real and imaginary part of the output impedance (transmitting BP4 with coupling)

5 Summary of the Design Procedure

Because the design procedure is rather complicated, it seems to be sensible to outline the required steps. Summarizing, the following procedure has been proposed.

- 1) Definition of the start parameters a , h , f_0 , B_0 .
- 2) Estimation of the reflection factor ρ_0 about B_0 using the Butterworth-Approximation for a BP4.
- 3) Correction of ρ_0 with condition $B \geq B_0$ and using the named formulae for the circuit elements.
- 4) Once again correction of ρ_0 , now looking at the entire circuit inclusive coupling between the band-pass filters. A circuit simulation program such as SPICE is recommended. The design formulae (13-15) be applied directly as parameter sets.
- 5) Determination of the element values.
- 6) Verification of the complete circuit, realization and practical tests may follow.

6 Another Example

If a higher bandwidth is required for an increased data transmission rate, a higher centre-frequency f_0 should be chosen. A candidate may be the ISM-frequency $f_0=13.56$ MHz taking into account the local regulations (e.g. see [6]). The other start parameters are $a=10$ cm, $h \approx 10$ cm, $B_0 \approx 500$ kHz with $L_a \approx 0.5$ μ H, $R_a \approx 0.5$ Ω , a coupling factor $k \approx 0.032$ and a mutual inductivity $M \approx 0.016$ μ H. The final results are the following: $L_1=L_6=3$ μ H, $C_2=C_5=57$ pF, $C_3=C_4=219$ nF; the filter curve (similar to a so-called Chebyshev band-pass) can

be seen in Figure 9 with $S_{21}^2(f)=P_2(f)/P_{1\max}$. A problem should be mentioned here regarding the definition of the bandwidth. Both cases are in use with $B=f_{c2}-f_{c1}$ and marked in Figure 9: $S_{21}^2(f_{c1,2})=S_{21}^2(f_0)/2$ and $S_{21}^2(f_{c1,2})=S_{21}^2(f_0)$. The second case is usually preferred about Chebyshev filters. In both cases, however, we have a considerable bandwidth suitable for higher data transmission rates and also advantageous concerning interference and other EMC aspects.

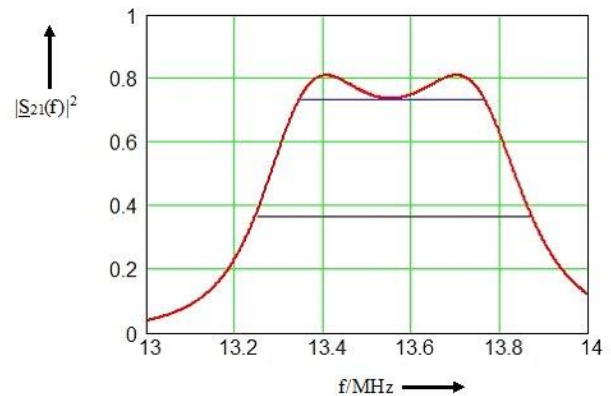


Fig. 9: Frequency-depending power transfer ($f_0=13.56$ MHz, $a=10$ cm, $h=10$ cm)

7 Conclusion

It is shown that the power transfer of two coupled inductive loops can be calculated, including two dedicated equal band-pass filters of 4th order. The loop properties, especially the shelf and mutual inductivity, given by the dimensions and the distance between the loops, have been taken into account, as well as the necessary bandwidth concerning the chosen data transmission rate. As final results, the frequency-depending power transfer functions have been calculated and plotted. The design procedure is rather complicated but has been described step by step whereby certain basics and the use of a circuit simulation program (here SPICE) are required. The design can be adapted to other requirements because all essential parameters are included. After having concentrated on the frequency behaviour here, future work will include the transient responses in detail.

References:

- [1] Transport modes. European Commission, [Online]. https://transport.ec.europa.eu/transport-modes_en (Accessed Date: October 11, 2024).

- [2] Eurobalise. DetailedPedia, [Online]. <https://www.detailedpedia.com/wiki-Eurobalise> (Accessed Date: October 11, 2024).
- [3] M.Vajdik, D. Komosny, I. Herman: Short-range Data Transmission Using Inductive Method. *WSEAS Transactions on Communications*, vol. 2 2003, pp. 190-193.
- [4] R. A. Gheorghiu, I. Badescu, R. S. Timnea: Infrastructure to vehicle communications using inductive loops. *WSEAS Transactions on Communications*, Vol. 13, 2014.
- [5] K. H. Kraft: Breitbandanpassung von Leiter-schleifen (Broadband Matching of Inductive Loops). *Frequenz* 52, 1998, 11/12, pp. 230-235.
- [6] P.Lathiya, J. Wang: Near-Field Communications (NFC) for Wireless Power Transfer (WPT): An Overview. IntechOpen, Open Access Chapter, from *Wireless Power Transfer- Recent Development, Applications and New Perspectives*, 2021.
- [7] W. Zhang, W. Niu, W. Gu: Experimental investigation of transfer characteristics of midrange underwater wireless power transfer. *PROOF- Int. J. of Appl. Science and Engin.*, Vol. 2, 2022, doi: 10.37394/232020.2022.2.19.
- [8] Y. Yamamoto, K. Yamaguchi, T. Hirata, I. Hodoka: Feedback effect for wireless high-power transmission. *WSEAS Transactions on Circuits and Systems*, Vol.13, 2014.
- [9] M. Thompson: Inductance Calculation Techniques. Part II. *Power Control and Intelligent Motion*, December 1999.
- [10] H. W. Bode: *Network Analysis and Feedback Amplifier Design*. Van Nostrand, New York 1956.
- [11] R. Saal, W. Entenmann: *Handbook of Filter Design*. Hüthig, Heidelberg 1973.

Contribution of Individual Authors to the Creation of a Scientific Article (Ghostwriting Policy)

The author contributed in the present research, at all stages from the formulation of the problem to the final findings and solution.

Sources of Funding for Research Presented in a Scientific Article or Scientific Article Itself

No funding was received for conducting this study.

Conflict of Interest

The author has no conflicts of interest to declare.

Creative Commons Attribution License 4.0 (Attribution 4.0 International , CC BY 4.0)

This article is published under the terms of the Creative Commons Attribution License 4.0

https://creativecommons.org/licenses/by/4.0/deed.en_US